Two-photon absorption spectra of direct and indirect materials: ZnO and AgCl

I. M. Catalano, A. Cingolani, and M. Lepore
Dipartimento di Fisica dell'Università di Bari, Unità Gruppo Nazionale Elettronica Quantistica Plasmi, Consiglio Nazionale delle Ricerche, Bari, Italy
(Received 30 December 1985)

The transition mechanisms actually involved in direct and indirect two-photon absorption (TPA) processes have been investigated in two different materials: ZnO and AgCl. It has been proven that the TPA dominant mechanism changes when the excitation energy is varied. In particular, in both materials and for both direct and indirect processes, transitions are of the allowed-allowed type near the energy gap and become of the allowed-forbidden type far from the gap.

In recent years much work has been done to critically compare the theoretical and experimental values of the direct ($\alpha_d^{(2)}$) and indirect ($\alpha_i^{(2)}$) two-photon absorption coefficients in order to obtain a better agreement between them.[1] In spite of this, the $\alpha_d^{(2)}$ and $\alpha_i^{(2)}$ theoretical values generally underestimate experimental data. This was initially ascribed to large errors ($\sim 50\%$) affecting the measurements. Later, improvements in experimental techniques greatly reduced errors, showing that the disagreement is probably due to approximations made in calculations. In fact, in the different theoretical evaluations of $\alpha_d^{(2)}$ and $\alpha_i^{(2)}$, the factors, which in all probability cause the lack of agreement, are (a) the squared values of dipole matrix elements, $|P_{ij}|^2$ (where i and j indicate the initial and final states, respectively), (b) the transition mechanism actually involved (allowed-allowed, allowed-forbidden), and (c) the state density uncertainty.

As regards $|P_{ij}|^2$, recent studies, carried out on different semiconductors by means of the ratio method,[2] have enabled a better understanding of the role of $|P_{ij}|^2$. In particular, they have shown that Kane's approximation is the most valid among the different ones available for the dipole matrix element, at least when its validity condition [excitation energy nearly resonant with the energy gap (E_g)] is respected. When this condition is neglected, that is the excitation energy is much larger than E_g, nothing can be said about $|P_{ij}|^2$. In fact, in this case, not only does $|P_{ij}|^2$ become dependent on the energy, but also the transition mechanism actually involved must be reconsidered. It has already been shown, for a small direct gap semiconductor (GaAs), that there is a change in the dominant transition mechanism when the excitation energy becomes larger than E_g.[3]

This paper reconsiders the problem in two different large-gap semiconductors (ZnO and AgCl) in order to analyze the transition mechanism actually involved, both in direct and in indirect two-photon processes.

For this purpose, the spectral dependence of the TPA coefficient near and far from the energy gap in both materials has been studied (for ZnO: 2 meV $\leq 2\hbar\omega - E_g \leq$ 710 meV; for AgCl: 174 meV $\leq 2\hbar\omega - E_g \leq$ 1220 meV, where $2\hbar\omega$ is the excitation energy).

Measurements have been carried out on ZnO and AgCl crystals. The former is a direct-gap semiconductor[4] ($E_g = 3.43$ eV, $m_c = 0.19 m_0$, $m_{v1} = 0.21 m_0$, $m_{v2} = 0.2 m_0$, $m_{v3} = 0.71 m_0$, $n = 2$) with a hexagonal structure. It has an s-like conduction band having a Γ_7 symmetry. The valence band is p-like, splitting into three degenerate bands due to spin-orbit and crystalline-field interactions. The top valence band has a Γ_9 symmetry while the two lower ones have a Γ_7 symmetry. AgCl is an indirect-gap ionic crystal[5] ($E_{gi} = 3.2$ eV, $\hbar\Omega = 0.024$ eV, $m_c = 0.3 m_0$, $m_v = m_0$, $n = 2.071$) for which band-structure calculations indicate the presence of two valence-band maxima having nearly the same energy, located at the L point (L_3) and on the Σ line (Σ_4) in the Brillouin zone. A conduction-band minimum of standard form is at the Γ point (Γ_1).

High-quality crystals were selected to prevent damage from high power-density excitation and to avoid dependence on the degree of sample purity. In particular, the AgCl samples were polished and annealed before measuring, as described by Stulen and Ascarelli.[6]

The $\alpha^{(2)}$ spectral dependence at 77 K for both ZnO and AgCl was obtained by means of the nonlinear luminescence experimental technique.[7] This consists of the detection of a luminescence signal L (at $\hbar\omega_L = 2.34$ eV for ZnO and at $\hbar\omega_L = 2.6$ eV for AgCl) excited by simultaneous absorption of two identical photons. The detected luminescence intensity L is given by[3]

$$L = \Delta I_{\mathrm{TPA}} q f(\omega_L/2\omega) \ , \tag{1}$$

where

$$\Delta I_{\mathrm{TPA}} = [\alpha^{(2)} I_0^2 z/(1+\alpha^{(2)} I_0^2 z)](1-\alpha^{(1)} z) \ ,$$

q is the quantum efficiency for excitation at $2\hbar\omega$, which is assumed to be constant over the energy range considered, f is the fraction of the collected luminescence which is a function of the geometry, and the other symbols have their usual meanings as reported in Ref. 3. The experimental setup was similar to that reported in Ref. 7.

The TPA spectra were obtained by means of a Quantel Datachrome dye laser (pulse duration: 9 nsec, maximum peak power for Rhodamine 6 G nearly equal to 30 MW/cm^2) pumped by the second harmonic of a pulsed YAlG-Nd laser. Three highly efficient dyes were used: Rhodamine 6 G for the high-energy side of the spectra, DCM for the intermediate region, and LD700 for the low energies. The quadratic behavior of the detected luminescence signal versus the excitation intensity was checked at each experimental point, and for each of them, different measurement runs were carried out. The experimental accuracy was within about 25% for each run.

The TPA spectrum for ZnO as a function of $(2\hbar\omega - E_g)$ is shown in Fig. 1. In the same figure the continuous curves *a* and *b* (calculated by the first two equations in Table I) are related to a three-band model[8] (allowed-allowed transitions) and a two-band model[9] (allowed-forbidden transitions), respectively. It is worthwhile to note that the first one is calculated in the parabolic band approximation, while the second uses the nonparabolic one.

In Fig. 1, for the three-band model [characterized by a $(2\hbar\omega - E_g)^{1/2}$ spectral dependence], accurate proportionality is found for $(2\hbar\omega - E_g)$ ranging between 10 and 120 meV above the band gap. However, in the initial region up to ~ 10 meV, the $\alpha_d^{(2)}$ values are greater than the calculated ones. This difference is due to exciton contribution in the continuum. To illustrate this more clearly, the experimental points in this range have been plotted on a linear scale in the Fig. 1 inset. The plot shows that the experimental points fit theoretical curve c well (calculated by the third equation of Table I), which gives the characteristic dependence on the exciton state density for $\alpha_d^{(2)}$. This behavior confirms the importance of the exciton effect in TPA processes for $2\hbar\omega \geq E_g$.[11]

On the other side, in the range beyond 120 meV above the band gap, a good agreement is found with curve b, given by the two-band model, which has an approximately $(2\hbar\omega - E_g)^{3/2}$ spectral dependence. This agrees with results previously obtained for other semiconductors with the excitation conditions $2\hbar\omega >> E_g$.[11]

Finally, the increase in $\alpha_d^{(2)}$ at $(2\hbar\omega - E_g) \cong 500$ meV can be attributed to transitions from a lower valence band Γ_7. It is worth noting that these transitions are forbidden to one-photon processes, as reported by other authors.[12]

These experimental results, in agreement with those reported in Ref. 3, yield definitive evidence that for direct-gap semiconductors the dominant transition mechanism is of the allowed-allowed type near the energy gap, while far from this, the allowed-forbidden contribution becomes preponderant. Moreover, these results reconfirm the importance of both nonparabolicity and degeneracy-band effects for $2\hbar\omega >> E_g$ and of the exciton state density for $2\hbar\omega \geq E_g$, in TPA processes.

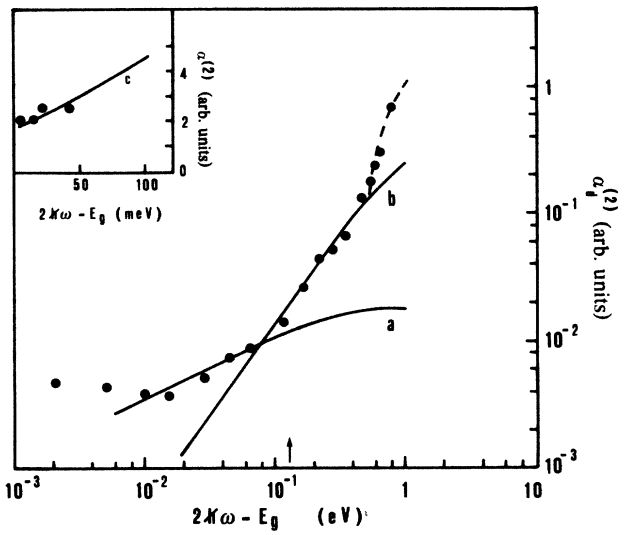

FIG. 1. Two-photon absorption coefficient vs $(2\hbar\omega - E_g)$ for a ZnO single crystal. Full lines a and b are calculated by means of the three- and two-band models, respectively. The inset shows the excitonic contribution (curve c) in the energy range between 10^{-3} and 10^{-2} eV. The symbols indicate experimental results. For the energy value indicated by the arrow $(2\hbar\omega - E_g = 0.13$ eV), $\alpha_d^{(2)}$ is equal to 0.021 cm MW^{-1} (Ref. 16).

TABLE I. Theoretical model calculations for two-photon direct transitions. Symbols have been defined in Refs. 8, 9, and 10.

Author	Model	Band structure	Transitions type	Result of calculation
Hassan (Ref. 8)	Three bands	Parabolic anisotropic bands	Allowed-allowed	$\alpha_d^{(2)} = \frac{2^{5/2}e^4\pi}{n^2c^2m^{5/2}} \frac{\lvert P_{cn}\rvert^2 \lvert P_{nv}\rvert^2}{(\hbar\omega)^3} (\alpha_c + \alpha_v)^{-1} \times \frac{1}{M(BM)^{1/2}} \left[\frac{X}{1+X^2} + \arctan X \right]$ $B = \left[(\beta_v + \beta_n) - \frac{\alpha_n + \alpha_v}{\alpha_c + \alpha_v} (\beta_c + \beta_v) \right]$ $X = \left[\frac{B(2\hbar\omega - E_g)}{M(\beta_c + \beta_v)} \right]^{1/2}$
Vaidyanathan *et al.* (Ref. 9)	Two bands	Nonparabolic bands	Allowed-forbidden	$\alpha_d^{(2)} = \frac{2^3\pi e^4}{3\epsilon_\infty C^2} \frac{E_g^{3/2}}{(m_{cv}^*)^{1/2}} \frac{1}{(\hbar\omega)^4} \left[\left[\frac{2\hbar\omega}{E_g} \right]^2 - 1 \right]^{3/2}$
Lee and Fan (Ref. 10)			Exciton	$\alpha_d^{(2)} = \frac{2^8\pi}{\sqrt{2}\times 15} \frac{e^4}{c^2m^4} \frac{\mu_0^{5/2}}{n} \frac{1}{(\hbar\omega)^3} \left[(1+X^2) \frac{\pi X e^{\pi X}}{\sinh(\pi X)} \frac{J^2 A}{X^3 E_b^{1/2}} \right]$ $A = P^2(ar^2 + b\rho_2^2 + c\rho_1^2\rho_2^2 + dr\rho_2 + er\rho_1\rho_2 + f\rho_1\rho_2^2)$

Figure 2 gives the TPA spectrum of AgCl. In this figure curves a and b (calculated by the first and second equations of Table II) are due to a four-band[11] and a three-band model,[12] respectively. In particular, the four-band model assumes that the main contributions are given by allowed virtual transitions, while the three-band model uses forbidden virtual ones. It is evident that, in the region nearer the indirect gap (174 meV $\leq 2\hbar\omega - E_g \leq$ 800 meV), the experimental points well fit the curve related to the four-band model, characterized by a spectral dependence roughly equal to $(2\hbar\omega - E_{gi} - \hbar\Omega)^2$. Beyond 800 meV above the indirect gap, the $\alpha_i^{(2)}$ values, in agreement with Casalboni, Crisanti, Francini, and Grassano,[15] fall along the three-band model curve. The latter is characterized by a spectral dependence approximately equal to $(2\hbar\omega - E_{gi} - \hbar\Omega)^3$.

These results show that, for indirect-gap materials also, the allowed-forbidden transitions dominate the two-photon processes for energies well above the indirect band gap, whereas it is the allowed-allowed transitions which dominate just above this gap.

In conclusion, we have demonstrated that, both in direct and indirect TPA processes, the dominant transition mechanism changes when the excitation energy is varied. This suggests that not only the role of state density, but also that of the different TPA transition mechanisms, related to direct and indirect gap, must be carefully reconsidered in order to improve the agreement between experimental and theoretical TPA coefficients.

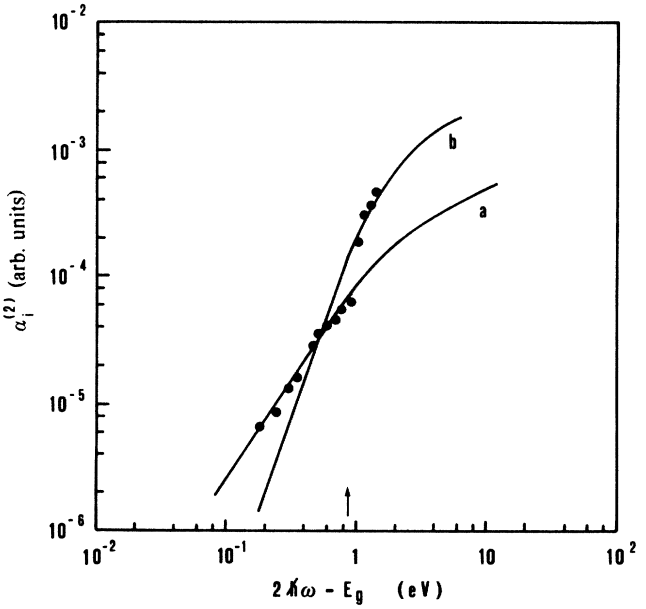

FIG. 2. Indirect two-photon absorption coefficient vs $(2\hbar\omega - E_{gi})$ for an AgCl sample. Full lines a and b are calculated by means of the four- and three-band model, respectively. The symbols indicate experimental results. For the energy value indicated by the arrow $(2\hbar\omega - E_{gi} = 0.9$ eV), $\alpha_i^{(2)}$ is equal to 1.25×10^{-4} cm MW^{-1} (Ref. 15).

TABLE II. Same as Table I for two-photon indirect transitions. Symbols have been defined in Refs. 13 and 14.

Authors	Model	Band structure	Transition type	Result of the calculations
Bassani (Ref. 13)	Four bands	Parabolic isotropic bands	Allowed-allowed	$\alpha_i^{(2)} = \frac{2e^4}{n^2c^2m\hbar^3}\frac{\lvert P_{mn}\rvert^2\lvert P_{nv}\rvert^2\lvert Q_{cm}\rvert^2}{(\hbar\omega)^3}(\alpha_c\alpha_v)^{-3/2} \times \sum_{+,-}\frac{(2\hbar\omega - E_i \mp \hbar\Omega)^2}{\mp(e^{\mp\hbar\Omega/kT}-1)} \times\left[\frac{1}{(\Delta m - E_i \mp\hbar\Omega)^2}\right]\left[\frac{1}{(\Delta n-\hbar\omega)^2}+\frac{1}{(\Delta n - E_i+\hbar\omega\mp\hbar\Omega)^2}\right] + \frac{1}{(\Delta n - E_i\mp\hbar\Omega)^2}\left[\frac{1}{(\Delta m-\hbar\omega)^2}+\frac{1}{(\Delta m - E_i+\hbar\omega\mp\hbar\Omega)^2}\right]\Bigg].$
Yee (Ref. 14)	Three bands	Parabolic isotropic bands	Allowed-forbidden	$\alpha_i^{(2)} = \frac{2^5e^6\pi m^2}{3n^2\hbar}\frac{\hbar\Omega}{(\hbar\omega_F)^2}\left(\frac{1}{\epsilon_\infty}-\frac{1}{\epsilon_0}\right)\frac{\lvert P_{cv}\rvert^2}{(\hbar\omega)^3}(\alpha_c\alpha_v)^{-3/2} \times\Bigg[\left(\frac{1}{\alpha_c}\lvert g_1^+\rvert^2+\frac{1}{\alpha_v}\lvert g_2^+\rvert^2\right)n_{kf}(2\hbar\omega+\hbar\Omega-E_i)^3 + \left(\frac{1}{\alpha_c}\lvert g_1^-\rvert^2+\frac{1}{\alpha_v}\lvert g_2^-\rvert^2\right)(n_{kf}+1)(2\hbar\omega-\hbar\Omega-E_i)^3\Bigg]$ $g_1^{\pm} \approx \left[\frac{\alpha_c}{m\hbar\omega}\left(\frac{1}{E_{k_f^v}-E_{k_0^v}\mp\hbar\Omega}+\frac{1}{E_{k_0^c}-E_{k_f^c}+\hbar\omega}\right) - \frac{\alpha_v}{m}\frac{1}{(E_{k_f^v}-E_{k_0^v}-\hbar\omega)(E_{k_f^v}-E_{k_0^v}\mp\hbar\Omega)}\right],$ $g_2^{\pm} \approx \left[\frac{\alpha_v}{m\hbar\omega}\left(\frac{1}{E_{k_0^c}-E_{k_f^c}\pm\hbar\Omega}+\frac{1}{E_{k_f^v}-E_{k_0^v}-\hbar\omega}\right) + \frac{\alpha_c}{m}\frac{1}{(E_{k_0^c}-E_{k_f^c}\pm\hbar\Omega)(E_{k_0^c}-E_{k_f^c}+\hbar\omega)}\right]$ $n_{kf} = \frac{1}{e^{\hbar\Omega/k_BT}-1}$

We are grateful to M. Sibilano for technical assistance in the experiment. This work was partially supported by Ministero della Pubblica Istruzione.

[1]I. M. Catalano, A. Cingolani, and M. Lepore, Solid State Commun. **54**, 87 (1985); I. M. Catalano and A. Cingolani, Phys. Rev. B **52**, 538 (1984); **28**, 1130 (1983); A. Vaidyanathan, T. Walker, A. H. Guenther, S. S. Mitra, and R. M. Narducci, *ibid.* **21**, 743 (1980); A. Vaidyanathan, A. H. Guenther, and S. S. Mitra, *ibid.* **24**, 2259 (1981), and references therein.

[2]I. M. Catalano, A. Cingolani, and M. Lepore, Solid State Commun. **55**, 151 (1985).

[3]J. P. van der Ziel, Phys. Rev. B **16**, 2775 (1977).

[4]Y. S. Park, C. W. Litton, T. C. Collins, and D. C. Reynolds, Phys. Rev. **143**, 512 (1966); V. V. Sobolev, V. I. Donetskikh, and E. F. Zagainov, Fiz. Tekh. Poluprovodn. **12**, 1089 (1978) [Sov. Phys. Semicond. **12**, 646 (1978)].

[5]R. B. Laibowitz and H. S. Sack, Phys. Status Solidi **17**, 353 (1966); M. N. Popova and I. Pelant, Phys. Status Solidi (b) **69**, 93 (1975); G. L. Bottger and C. V. Damsgard, Solid State Commun. **9**, 1277 (1971).

[6]R. H. Stulen and G. Ascarelli, Phys. Rev. B **15**, 1161 (1977).

[7]I. M. Catalano and A. Cingolani, J. Appl. Phys. **50**, 5638 (1978).

[8]A. R. Hassan, Nuovo Cimento **70B**, 21 (1970).

[9]A. Vaidyanathan, A. H. Guenther, and S. S. Mitra, Phys. Rev. B **22**, 6480 (1980).

[10]C. C. Lee and H. F. Fan, Phys. Rev. B **9**, 3502 (1974).

[11]I. M. Catalano and A. Cingolani, Phys. Rev. B **19**, 1049 (1979).

[12]G. Pensl, Solid State Commun. **11**, 1277 (1972); G. Koren, Phys. Rev. B **11**, 802 (1975).

[13]F. Bassani and A. R. Hassan, Nuovo Cimento **7B**, 313 (1972).

[14]J. H. Yee, J. Phys. Chem. Solids **33**, 643 (1972).

[15]M. Casalboni, F. Crisanti, R. Francini, and U. M. Grassano, Solid State Commun. **35**, 833 (1980).

[16]G. Kobbe and C. Klingshirn, Z. Phys. B **37**, 9 (1980).